Pergamon

Bioorganic & Medicinal Chemistry 10 (2002) 261–268

BIOORGANIC & MEDICINAL CHEMISTRY

Kinetic and Crystallographic Studies of Glucopyranosylidene Spirothiohydantoin Binding to Glycogen Phosphorylase B

Nikos G. Oikonomakos,[a,*] Vicky T. Skamnaki,[a] Erzsébet Ösz,[b] László Szilágyi,[b] László Somsák,[b] Tibor Docsa,[c] Béla Tóth[c] and Pál Gergely[c]

[a]*Institute of Biological Research and Biotechnology, The National Hellenic Research Foundation, 48 Vas. Constantinou Avenue, Athens 11635, Greece*

[b]*Department of Organic Chemistry, University of Debrecen, POB 20, H-4010 Debrecen, Hungary*

[c]*Department of Medical Chemistry, Medicaland Health Science Centre, University of Debrecen, H-4026 Debrecen, Bem ter 18/B, Hungary*

Received 11 May 2001; accepted 25 July 2001

Abstract—Glucopyranosylidene spirothiohydantoin (TH) has been identified as a potential inhibitor of both muscle and liver glycogen phosphorylase b (GPb) and a (GPa) and shown to diminish liver GPa activity in vitro. Kinetic experiments reported here show that TH inhibits muscle GPb competitively with respect to both substrates phosphate ($K_i = 2.3$ μM) and glycogen ($K_i = 2.8$ μM). The structure of the GPb–TH complex has been determined at a resolution of 2.26 Å and refined to a crystallographic R value of 0.193 ($R_{free} = 0.211$). The structure of GPb–TH complex reveals that the inhibitor can be accommodated in the catalytic site of T-state GPb with very little change of the tertiary structure, and provides a basis of understanding potency and specificity of the inhibitor. The glucopyranose moiety makes the standard hydrogen bonds and van der Waals contacts as observed in the glucose complex, while the rigid thiohydantoin group is in a favourable electrostatic environment and makes additional polar contacts to the protein.

Introduction

Glycogen phosphorylase (GP) catalyses the degradative phosphorolysis of glycogen to glucose 1-phosphate (Glc-1-P). In muscle, Glc-1-P is utilised via glycolysis to generate metabolic energy, and in the liver it is converted to glucose.[1] The enzyme exists in two interconvertible forms: the dephosphorylated form, GPb, and the phosphorylated form, GPa. In resting muscle the enzyme exists in the inactive form (GPb), which can be activated either by non-covalent co-operative binding of AMP (or IMP) or by covalent phosphorylation to form GPa. Both forms can exist in a less active T state and a more active R state according to the Monod–Wyman–Changeux model for allosteric proteins.[2] The R state is induced by AMP (or IMP), substrates or certain substrate analogues and the T state is stabilised by the binding of ATP, Glc-6-P, glucose and caffeine.[3–5]

Because of its central role in glycogen metabolism, GP has been exploited as a target for structure-assisted design of compounds that might prevent unwanted glycogenolysis under high glucose conditions that may be relevant to the control of diabetes. An understanding of how these inhibitors bind to the enzyme should provide a rational basis for the development of new molecules with an increased affinity and specificity for GP. Several binding sites, for example the catalytic, the allosteric, and the inhibitor sites, have been identified as targets for inhibitor binding and protein crystallography has contributed significant information on the specificity and interactions that distinguish the binding sites and also revealed unexpected binding sites.[6–18]

The catalytic site has been probed with glucose and glucose analogues inhibitors. A systematic work involving structure-assisted design, synthesis, kinetic characterisation, and X-ray crystallographic binding studies has led to the discovery of over 80 glucose analogues inhibitors of GPb with similar kinetic and structural characteristics.[6–10,12,19] The common kinetic and

*Corresponding author. Tel.; +30-1727-3761; fax: +30-1727-3758; e-mail: ngo@eie.gr

0968-0896/02/$ - see front matter
PII: S0968-0896(01)00277-2

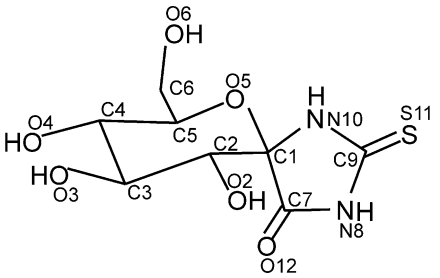

Scheme 1. Glucopyranosylidene spirothiohydantoin structure, showing the numbering system used.

structural features of these compounds is that they are highly selective for GPb, they are competitive inhibitors with respect to the substrate Glc-1-P, and they bind at the catalytic site by stabilising the T-state enzyme.

Glucopyranosylidene spirohydantoin (H) is the most effective glucose analogue inhibitor for GPb with a $K_i = 3.1$ μM,[8] more than 500 times lower than the corresponding K_i (1.7 mM) for glucose.[6] H binds at the catalytic site with the spirohydantoin group filling the empty space at the β configuration adjacent to C1 of glucopyranose as defined previously.[6] In an attempt to fill the space available in the position O11 (see Scheme 1) with a group that was nonpolar but easily polarised we found that TH was indeed a good competitive inhibitor ($K_i = 5.1$ μM) with respect to Glc-1-P. Assays with muscle and liver GPb and GPa enzyme render TH and H to be equipotent inhibitors. [20,21] However, the synthetic routes to H are rather lengthy (almost 10 or more steps from an easily available precursor or the free sugar) or give much less efficient inhibitor as the major product. The synthesis of TH has been reported previously[20] and it has been demonstrated that TH, contrary to H, can be produced in gram amounts,[22] thereby facilitating more sophisticated biological studies to be carried out.[23]

In this work, we demonstrate through kinetic studies that TH has a similar potency on rabbit muscle enzyme in the direction of glycogen breakdown to that observed in the direction of glycogen synthesis. We have also determined the structure of the GPb-TH complex by X-ray crystallographic methods at 2.26 Å resolution. The structural results show that TH binds at the catalytic site in a similar position to that occupied by H and mimicks the contacts of H that stabilise the closed position of the 280s loop (residues 282–286).

Results and Discussion

Kinetics

Inhibition constants of TH for muscle and liver GPb and GPa assayed into the direction of glycogen synthesis have been reported previously.[20,21] The inhibitory efficiency of TH was also tested with GPb assayed into the direction of glycogen breakdown. The physiologically relevant assay conditions proved that TH is a very potent inhibitor of muscle glycogen phosphorylase b (Fig. 1a and b). The K_i values for both substrates, $K_i = 2.8 \pm 0.3$ μM, with respect to varying glycogen concentrations, and $K_i = 2.3 \pm 0.3$ μM, with respect to varying Pi concentrations, respectively, are in agreement with the previously published K_i (5.1 ± 0.1 μM) determined into the direction of glycogen synthesis.

X-ray crystallography

The overall architecture of the native T-state GPb with the location of the catalytic site, the allosteric site, the inhibitor site, and a novel allosteric site that has been described previously[17] is presented in Fig. 2. The two subunits of the functionally active dimer are related by a crystallographic 2-fold symmetry axis. A summary of the data processing statistics and refinement parameters for the GPb–TH complex structure is given in Table 1. The structure of the GPb-TH complex has been refined at 2.26 Å to a crystallographic R value 0.193 ($R_{free} = 0.211$) (Table 1). TH binds at the catalytic site which is buried some 15 Å from the surface of the enzyme at the bottom of a long channel.

Table 1. Summary of diffraction data and refinement statistics for T-state GPb–TH complex

Space group	$P4_32_12$
No. of images (°)	58 (46.4°)
Unit cell dimensions	$a = b = 128.8$ Å, $c = 116.2$ Å
Resolution range	30–2.26 Å
No. of observations	255,617
No. of unique reflections	45,104
$I/\sigma(I)$ (outermost shell)	17.5 (5.5)
Completeness (outermost shell)	97.4% (99.9%)
R_m (outermost shell)	0.041 (0.158)
Multiplicity	3.8
Outermost shell	2.30–2.26 Å
Mosaicity	0.25
Refinement (resolution)	28.06–2.26 Å
No of reflections used (free)	42,768 (2278 free)
Residues included	13–842
No of protein atoms	6749
No of water molecules	243
No of ligand atoms	15 (PLP)
	17 (TH)
Final R (R_{free})	19.3% (22.1%)
RMSD in bond lengths (Å)	0.008
RMSD in bond angles (°)	1.4
RMSD in dihedral angles (°)	25.4
RMSD in improper angles (°)	0.75
Average B (Å^2) for protein residues	13–842
Overall	34.6 (30.8)*
CA,C,N.O	33.1 (29.3)*
Side chains	36.0 (32.3)*
Average B (Å^2) for ligands	
PLP	19.6
TH	18.6
Water	38.3

Merging R_m is defined as $R_m = \Sigma_i \Sigma_h \mid <I_h> - I_{ih} \mid / \Sigma_i \Sigma_h I_{ih}$, where $<I_h>$ and I_{ih} are the mean and ith measurement of intensity for reflection h, respectively. $\sigma(I)$ is the standard deviation of I. Crystallographic R factor is defined as $R = \Sigma \mid |F_o| - |F_c| \mid / \Sigma |F_o|$, where $|F_o|$ and $|F_c|$ are the observed and calculated structure factor amplitudes, respectively. R_{free} is the corresponding R value for a randomly chosen 5% of the reflections that were not included in the refinement. *Average B (Å^2) is given in parentheses for protein residues if the poorly defined residues (13–16, 209–212, 250–260, 313–326, 548–557, 831–842) were excluded. RMSD is the root-mean-square deviation.

TH binding site

The electron density difference map (against native T-state GPb) showed a strong positive peak representing binding of TH, and concomitant changes of the enzyme, normally observed on binding glucose or glucose analogues at the catalytic site,[6,9,24] indicating a small movement of His377 away from the sugar in order to optimise contacts to O6 and displacement of four water molecules. Views of the final $2F_o$–F_c electron density map for the TH molecule itself and in complex with GPb are shown in Figure 3a and b.

The electron density suggests that TH is tightly bound to the enzyme, consistent with the kinetic results (ref 20 and this work). TH could be fitted unambiguously, since clear density was present for all atoms of the inhibitor. In addition, after refinement of the protein and TH atoms, the position of the sulphur atom (S11) was apparent as the highest peak in the difference Fourier synthesis. The final refinement gave an average *B*-factor of 18.6 Å^2 for the TH molecule.

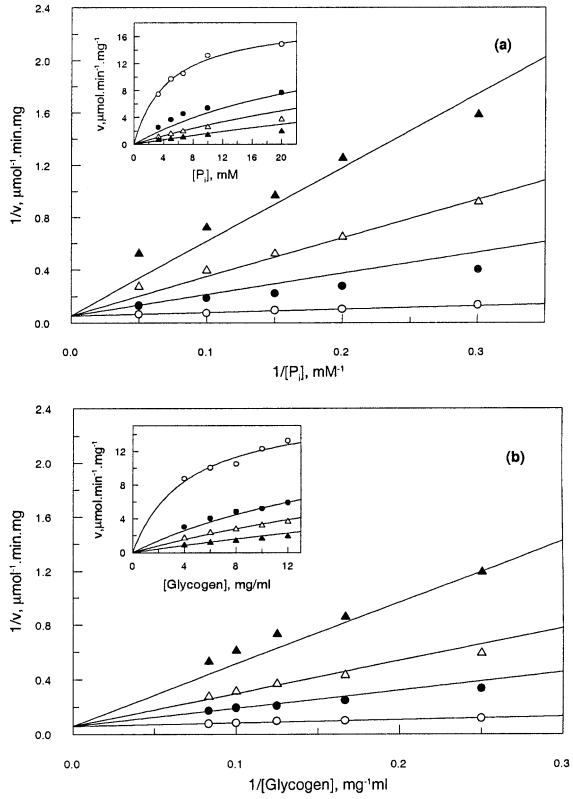

Figure 1. Kinetics of glucopyranosylidene spirothiohydantoin (TH) inhibition of GPb. (a) Double reciprocal plots of initial reaction velocity versus [P_i] at constant concentration of glycogen (10 mg/mL), and varying concentrations of phosphate (3.33–20 mM). Concentrations of TH were as follows: 0 (○), 12.5 (●), 25 (△), and 50 μM (▲) . Best fit lines were computer generated according to the equation for competitive inhibition (Grafit) by fitting all of the data at once. The kinetic parameters determined by this method are as follows: $K_m = 4.7 \pm 0.9$ mM, $V = 18.5 \pm 1.2$ U/mg, $K_i = 2.3 \pm 0.3$ μM . Inset: Fit of the calculated lines to the initial rate measurements. (b) Double reciprocal plots of initial reaction velocity versus [glycogen] at constant concentration of phosphate (20 mM), and varying concentrations of glycogen (4-12 mg/mL). Concentrations of TH were as follows: 0 (○), 12.5 (●), 25 (△), and 50 μM (▲). Best fit lines were computer generated as in (a). The calculated kinetic parameters are as follows: $K_m = 4.2 \pm 0.7$ mM, $V = 17.2 \pm 1.0$ U/mg, $K_i = 2.8 \pm 0.3$ μM. Inset: Fit of the calculated lines to the initial rate measurements.

Interactions between TH and catalytic site residues

The mode of binding of TH with GPb resembles that of H with GPb previously reported for room temperature[8] and 100 K GPb–H complex structures.[12] The glucopyranose moiety of TH makes the standard hydrogen bonds and van der Waals contacts as observed previously for glucose.[24] The amide nitrogen (N10) makes a hydrogen bond to the main-chain O of His377, an interaction that was observed for the β-D-*N*-acetyl-glucopyranosylamine.[9,10] In the GPb–TH complex, the hydrogen bond to N8 is maintained, but it is longer (3.4 Å) than in the GPb–H complex (3.1 Å). The hydrogen bonds to O12 are also maintained in both complexes, but TH forms an additional hydrogen bond between O12 and main-chain N of Gly135. In the GPb–H complex, O11 makes a rather weak hydrogen bond to ND2 of Asn284 (3.4 Å) and an indirect hydrogen bond to OD1 Asp339 through a water molecule (Wat10). In the GPb–TH complex, S11 makes 6 van der Waals contacts to Asn284 and to a water molecule (Wat10).

TH, on binding to GPb, makes a total of 15 hydrogen bonds — an additional rather long hydrogen bond (3.4 Å) is made between the N8 and ND2 atom of Asn284- and 67 van der Waals interactions (3 nonpolar/nonpolar, 13 polar/polar, and 45 polar/nonpolar). The

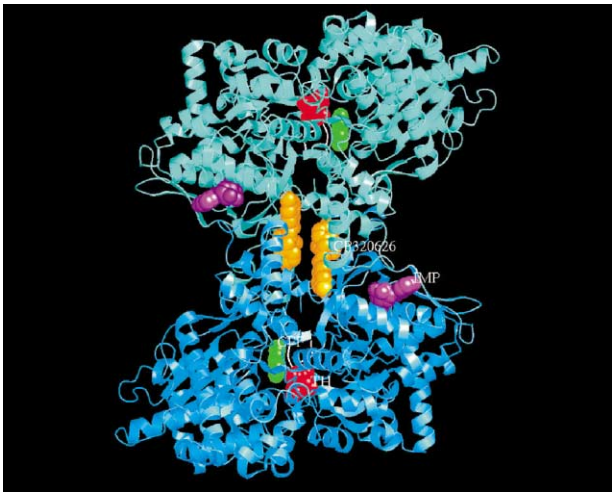

Figure 2. A schematic view of the GPb dimeric molecule viewed down the molecular dyad. The catalytic site, which includes the essential cofactor pyridoxal phosphate (PLP) (not shown), is buried at the centre of the subunit accessible to the bulk solvent through a 15 Å long channel. Glucopyranosylidene spirothiohydantoin (shown in red) binds at this site and promotes the less active T state through stabilisation of the closed position of the 280s loop (shown in white). The allosteric site, which binds the activator AMP, the weak activator IMP (shown in magenta), and other phosphorylated compounds, is situated at the subunit–subunit interface some 30 Å from the catalytic site. The inhibitor site, which binds purine compounds such as caffeine (CFF, shown in green), is situated at the entrance to the catalytic site tunnel, formed by two hydrophobic residues of Phe285 and Tyr613. The CP320626 binding site, located inside the central cavity formed on association of the two subunits, binds CP320626 molecule (shown in orange) and is some 15 Å from the allosteric effector site, 33 Å from the catalytic site and 37 Å from the inhibitor site.[17]

hydrogen bond interactions formed between the ligand and the protein are illustrated in Fig. 4. The structural results show that sulphur can be accommodated in this position with essentially no disturbance of the structure. There are no changes at the allosteric site, at the inhibitor site or at the tower/tower subunit interface.

Comparisons between GPb–TH and T-state GPb–H complex structures

The crystallographic analysis of the room temperature GPb–H complex, in which H was diffused into preformed crystals has been reported at a resolution of 2.4Å.[8] The structure of the GPb–H complex was further refined by applying solvent mask correction and including all data between 15 and 2.36 Å. The LSQKAB[25] superposition of the structure of the room temperature T-state GPb–H with the refined GPb–TH complex structure over well defined residues 17–208, 213–249, 261–312, 327–547 and 558–830 gave RMSDs of 0.066, 0.083, and 0.132 Å for Cα, main chain, and side-chain atoms, respectively, indicating that the two structures have very similar overall conformations to within the limits of the 2.26 Å resolution data and do not differ significantly at the interfaces between monomers. Similarly, the LSQKAB superposition of the 100K T-state GPb–H[12] and GPb–TH structures over well defined regions (residues 17–208, 213–249, 261–312, 327–547 and 558–830) gave RMSDs of 0.287, 0.307, and 1.045 Å for Cα, main-chain and side-chain atoms, respectively. A comparison of the positions of TH and H at the catalytic site is shown in Figure 5.

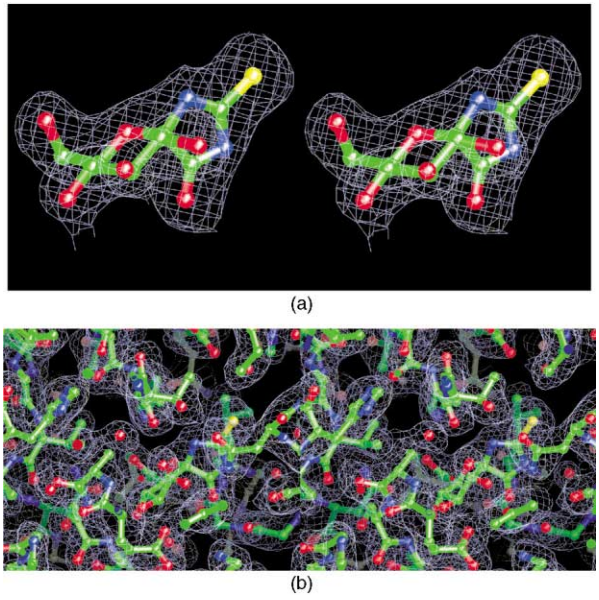

Figure 3. Electron density maps of the GPb–glucopyranosylidene spirothiohydantoin complex structure. Stereo diagrams of the glucopyranosylidene spirothiohydantoin molecule (*a*), and the catalytic site of the refined GPb-glucopyranosylidene spirothiohydantoin complex (*b*), showing bound glucopyranosylidene spirothiohydantoin and electron densities from the final weighted $2F_o$–F_c map, contoured at 1σ.

Potency and specificity

The structure of the GPb–TH complex pinpoints specific interactions responsible for the high affinity and specificity of TH for the enzyme. The hydrogen bonding network to the peripheral hydroxyls of the glucopyranose moiety of TH is analogous to that observed for the glucose complex.[24] Inhibitor binding occurs with the displacement of four water molecules. The increase in entropy from the release of these waters, together with the specific hydrogen bonds and van der Waals interactions (Table 2) appear to be the major source of binding energy that results in an inhibitor with μM affinity for GPb. The rigid planar nature of the substituent group suggests that there is little conformational energy change on binding, a further favourable factor. In native T-state enzyme there is no access from the buried catalytic site to the surface. Access to this site is partly blocked by the 280s loop in the T-state enzyme.[3] On transition from T-state to R-state, the 280s loop becomes disordered and displaced, thus opening a channel that allows substrate (glycogen) access to the catalytic site. The shift and disordering of the 280s loop is associated with changes at the intersubunit contacts of the dimer that give rise to allosteric effects.[4] The refined structure of the GPb–TH complex shows that TH, by making a hydrogen bond, through its O-2 hydroxyl, to Asn 284, 10 van der Waals contacts,

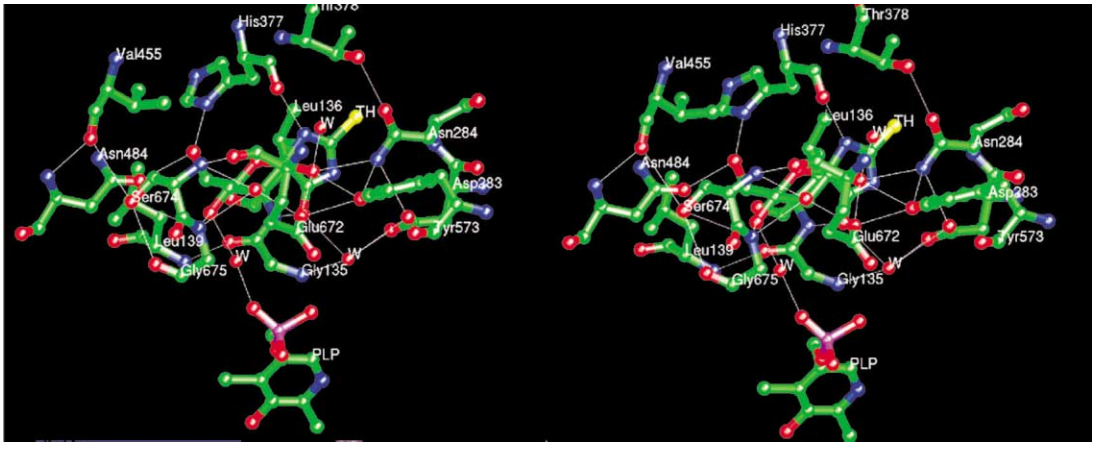

Figure 4. Binding mode of glucopyranosylidene spirothiohydantoin to GPb. Contacts between glucopyranosylidene spirothiohydantoin and GPb residues of the catalytic site.

Table 2. Hydrogen bonds and van der Waals contacts between glucopyranosylidene spirothiohydantoin and residues of the catalytic site of GPb A.

Inhibitor atom	Protein atom	Distance (Å)
Hydrogen bonds[a]		
O2	Asn284 ND2	2.9
	Tyr573 OH	3.1
	Glu672 OE1	3.2
	Wat102	2.8
O3	Glu672 OE1	2.6
	Ser674 N	3.1
	Gly675 N	3.0
O4	Gly675 N	2.8
	Wat131	2.5
O6	His377 ND1	2.6
	Asn484 OD1	2.8
N10	His377 O	2.9
N8	Asn284 ND2	23.4
012	Gly135 N	3.2
	Leu136 N	3.2
	Wat69	2.8

B. Van der Waals contacts

Inhibitor atom	Protein atom	No. of contacts
C1	His377 O	1
C2	His377 O;Glu672OE1; Wat 102	3
O2	Asn284 OG	1
C3	Glu672 OE1; Gly675 N; Wat 131	3
O3	Glu672 C, CG, CD; Ala673 C,CA, CB, N; Ser674 C, CA; Gly675 CA; Wat 102	11
C4	Asn484 OD1; Gly675 N; Wat 131	3
O4	Asn484 OD1; Ser674 C, CB; Gly675 C, CA, O	6
C5	Gly135 C; Leu136 N; Wat131	3
C6	Gly135 O; Leu139 CD2; His377 ND1; Asn484 OD1	4
O6	Leu139 CD2; His377 CG, CE1; Val455 CB, CG1, CG2; Asn484 Cg	7
O5	Leu136 N; His377 CB,O,ND1	4
N10	Asn284ND2; His377 C, CB	3
C9	Asn284 CG, ND2	2
S11	Asn284 CA, CG, N, OD1 ND2; Wat 10	6
N8	Asp283 OD1,OD2; Wat59; Wat 165	4
C7	Leu136 N; Asn284 ND2; Wat59	3
O12	Gly135 C, CA; Wat131	3
Total		67

[a]Wat102 is hydrogen bonded to Thr671 O (3.0 Å) and to Ala673 N (3.2 Å); Wat131 is in turn hydrogen bonded to Thr676 N (2.8 Å) and OG1 (3.2 Å); Wat59 is hydrogen bonded to Gly135 N (3.0 Å), to Asp283 OD1 (2.8 Å) and OD2 (3.2 Å), and to Arg569 N (2.7 Å) and Lys574 (3.2 Å) through another water molecule (Wat63).

through its O2, N10, C9, S11 and C7, to Asn284, and 2 van der Waals contacts, through its N8, to Asp283, stabilises the geometry of the 280s loop occurring in the T-state GPb because it interacts with residues from this loop, therefore inhibiting access of the substrate to the catalytic site.

In conclusion, the structural results show that sulphur can be accommodated in the catalytic site, and in particular, in the empty pocket in the β-configuration of C1 with essentially no disturbance of the structure. The gram-scale availability of TH and its promising biological effects [22,23] indicate that this compound can be of potential use in controlling hyperglycemia. Furthermore, knowing the details of TH interactions with the enzyme may help in the design of more potent and selective related inhibitors by making chemical modifications to the spirothiohydantoin ring.

Materials and Methods

Materials

GPb was isolated from rabbit skeletal muscle according to the method of Fischer and Krebs[26] with

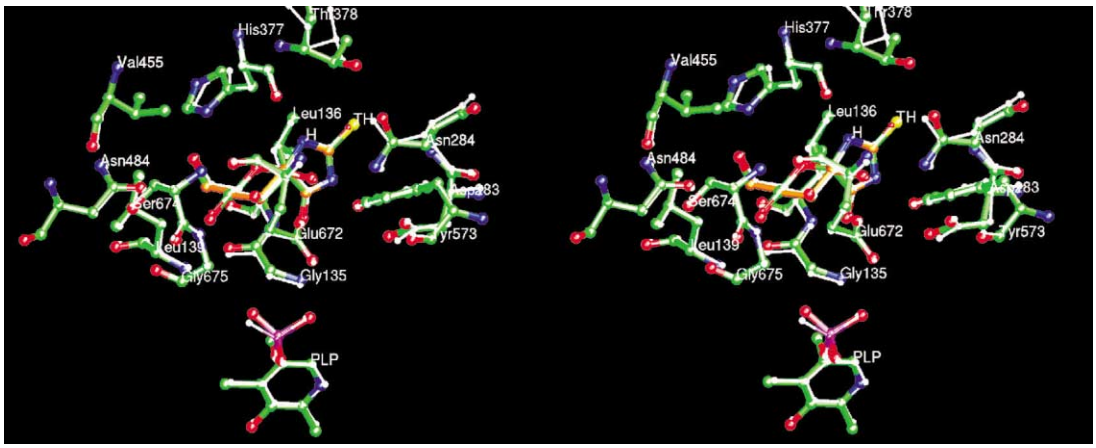

Figure 5. Comparison of the structures of the GPb–glucopyranosylidene spirothiohydantoin complex with the GPb-glucopyranosylidene spirohydantoin. Superposition of residues from the catalytic site in GPb. The view is similar to that of Fig. 4. The GPb-glucopyranosylidene spirothiohydantoin complex structure (green) with that of the 100K T-state GPb–glucopyranosylidene spirohydantoin white) complex structure are shown superimposed in stereo.

the difference of using 2-mercaptoethanol instead of L-cysteine. Phosphoglucomutase and glucose 1,6-bisphosphate were obtained from Boehringer Mannheim GmbH, glucose-6-phosphate dehydrogenase and AMP from Sigma. All other chemicals were purchased from Reanal (Hungary).

Assay of GPb activity

Enzyme activity was assayed in the physiological direction of glycogen breakdown. The assay mixture contained 50 mM pipes (pH 6.8), 10 μg/mL muscle GPb, 0.4 mM NADP, 10 μM glucose 1,6-bisphosphate, 2.5 mM magnesium-acetate, 4 U/mL phosphoglucomutase (NH_4^+-free, dialyzed 18 h against 50 mM sodium acetate, pH 5.3), 10 U/mL glucose-6-phosphate dehydrogenase (NH_4^+-free, dialyzed 18 h against 50 mM pipes, pH 6.8) and appropriate concentrations of glucopyranosylidene-spiro-thiohydantoin (TH) inhibitor. Control experiments demonstrated that TH did not influence the activities of coupling enzymes. For assays intended for calculation of K_i, fixed concentration of glycogen (10 mg/mL) and varying concentrations of phosphate (3.33–20 mM) or fixed concentration of phosphate (20 mM) and varying concentrations of glycogen (4–12 mg/mL) were used. The rate of enzyme-catalyzed reaction was monitored by absorbance measurements at 340 nm and 30 °C due to the formation of NADPH. Kinetic data were analyzed by the use of the nonlinear regression program GraFit.[27]

Crystallisation, data collection and processing

Tetragonal crystals of GPb were grown under conditions similar to those described previously,[28] except that the weak activator IMP was not added in the crystallisation medium. Prior to data collection at room temperature, a crystal was mounted in a thin-walled glass capillary and soaked for approximately 1 h in a freshly prepared buffered solution (10 mM Bes, 0.1 mM EDTA, 0.02 % sodium azide, pH 6.7) containing 70 mM TH. Data for GPb–TH complex were collected from a single crystal on an image plate RAXIS IV using a Rigaku Ru-H3RHB belt drive rotating anode ($\lambda = 1.5418$ Å), operating at 60 kV, 100 mA. The crystal to image plate distance was set at 180 mm to give a maximum resolution of 2.26 Å at the edge of the detector. Data frames of 0.8° oscillation angle were collected over total angular ranges of 46.4°. Crystal orientation and integration of reflections were performed using DENZO.[29] Inter-frame scaling, partial reflection summation, data reduction and post-refinement were all completed using SCALEPACK.[29]

Structure refinement

Crystallographic refinement of the GPb–TH complex was performed with X-PLOR version 3.8[30] using bulk solvent corrections. All data between 28.06 and 2.26 Å were included with no sigma cut-offs. Throughout the refinement, 5% of the data were flagged for calculation of R_{free}. The starting protein structure was the refined model of the room temperature GPb–H complex (see below). The Fourier maps calculated with SIGMAA[31] weighted (F_o–F_c) and ($2F_o$–F_c) coefficients indicated tight binding of TH at the catalytic site. A model of TH generated using the programme SYBYL [Tripos Associates Inc. (1992) SYBYL Molecular Modelling Software, St Louis, MO, USA] was fitted to the electron density map. Map interpretation was performed using the program O.[32] Several side chains of the enzyme model were adjusted and additional water molecules were added to the atomic model and retained only if they met stereochemical requirements by using WATERPICK (in X-PLOR). The final model was then refined by the conventional positional and restrained individual *B*-factor refinement protocol in X-PLOR 3.8 to give a final *R* factor value of 19.3% ($R_{free} = 22.1\%$). The final structure contained residues 13-842 and 256 water molecules. The first 12 N-terminal residues were not visible; this is true for all other reported structures of T-state GPb and GPb complexes. A Luzatti plot,[33] determined by using XPLOR 3.8 protocol, suggests an average positional error of approximately 0.25 Å. The Ramachandran plot[34] showed 87.3% of residues to be in the most favoured regions.

Refinement of the room temperature GPb–H complex, by using the structure of the GPb–glucose complex (PDB accession 2GPB) as a starting model for X-PLOR (version 3.1),[30] to a crystallographic R value of 0.177 for data between 8.0 and 2.4 Å, was summarised previously.[8] Further crystallographic refinement of the GPb–H complex was performed using the version 3.8 of the X-PLOR by applying solvent mask correction and including all reflections between 15 and 2.36 Å. In brief, the crystallographic R value for 31,588 reflections is 0.189 ($R_{free}=0.233$) and the current model, comprising residues 13–842, consists of 6749 protein atoms, 32 ligand atoms, and 220 water molecules. The RMSDs from ideal bond lengths and angles are 0.008 Å and 1.4°, respectively. The average B-factors for main-chain atoms, side-chain atoms, PLP, H, and water molecules were 30.1, 33.6, 20.0, 23.7, and 38.5 Å^2, respectively, if residues that exceeded 60 Å^2 (13–22, 209–211, 250–261, 314–326, 548–557, and 831–842) were excluded.

The structures were analysed with the graphics program O.[32] Hydrogen-bonds were assigned if the distance between the electronegative atoms was less than 3.3 Å and if both angles between these atoms and the preceding atoms were greater than 90°. Van der Waals interactions were assigned for non-hydrogen atoms separated by less than 4 Å. The protein structures were compared using either the LSQ option in O[32] or LSQKAB.[25]

Coordinates for T-state GPb–H and GPb–TH complexes have been deposited with the RCSB Protein Data Bank (http://www.rcsb.org/) (codes 1GGN, and 1HLF, respectively).

Acknowledgements

This work was supported by a Joint Research and Technology project between Greece and Hungary (2000–2002) (to N.G.O. and P.G.), Hungarian Scientific Research Fund (OTKA T26541), Hungarian Ministry of Health (ETT 01/2000), Hungarian Ministry of Education (FKFP 423/2000), Zsigmond Diabetes Foundation (Hungary), SRS Daresbury Laboratory (HPRI-CT-1999-00012), and EMBL, Hamburg Outstation (HPRI-CT-1999-00017). We wish to acknowledge the assistance of Irene Mavridis, Stella Makedonopoulou and Nikos Pinotsis, at the National Center for Scientific Research "Demokritos", Athens, Greece, for providing excellent facilities for data collection, and Katerina Tsitsanou and Spyros Zographos for their contribution to the project. Figures were produced using XOBJECTS, a molecular illustration programme (M.E.M. Noble, unpublished results).

References and Notes

1. Newgard, C. B.; Hwang, P. K.; Fletterick, R. J. *Crit. Rev. Biochem. Mol. Biol.* **1989**, *24*, 69.
2. Monod, J.; Changeux, J. P.; Jacob, F. *J. Mol. Biol.* **1965**, *12*, 88.
3. Johnson, L. N.; Hajdu, J.; Acharya, K. R.; Stuart, D. I.; McLaughlin, P. J.; Oikonomakos, N. G.; Barford, D. In *Allosteric Enzymes;* Herve, G., Ed.; CRC: Boca Raton, FL, 1989: p. 81.
4. Johnson, L. N. *FASEB J.* **1992**, *6*, 2274.
5. Oikonomakos, N. G.; Acharya, K. R.; Johnson, L. N. In *Post-translational Modification of Proteins;* Harding, J.J., Crabbe, M.J.C., Eds.; CRC: Boca Raton, FL, 1992; p. 81.
6. Martin, J. L.; Veluraja, K.; Johnson, L. N.; Fleet, G. W. J.; Ramsden, N. G.; Bruce, I.; Oikonomakos, N. G.; Papageorgiou, A. C.; Leonidas, D. D.; Tsitoura, H. S. *Biochemistry* **1991**, *30*, 10101.
7. Watson, K. A.; Mitchell, E. P.; Johnson, L. N.; Son, J. C.; Bichard, C. J. F.; Orchard, M. G.; Fleet, G. W. J.; Oikonomakos, N. G.; Leonidas, D. D.; Kontou, M.; Papageorgiou, A. C. *Biochemistry* **1994**, *33*, 5745.
8. Bichard, C. J. F.; Mitchell, E. P.; Wormald, M. R.; Watson, K. A.; Johnson, L. N.; Zographos, S. E.; Koutra, D. D.; Oikonomakos, N. G.; Fleet, G. W. J. *Tetrahedron Lett.* **1995**, *36*, 2145.
9. Oikonomakos, N. G.; Kontou, M.; Zographos, S. E.; Watson, K. A.; Johnson, L. N.; Bichard, C. J. F.; Fleet, G. W. J.; Acharya, K. R. *Protein Sci.* **1995**, *4*, 2469.
10. Watson, K. A.; Mitchell, E. P.; Johnson, L. N.; Cruciani, G.; Son, J. C.; Bichard, C. J. F.; Fleet, G. W. J.; Oikonomakos, N. G.; Kontou, M.; Zographos, S. E. *Acta Crystallogr.* **1995**, *D51*, 458.
11. Zographos, S. E.; Oikonomakos, N. G.; Tsitsanou, K. E.; Leonidas, D. D.; Chrysina, E. D.; Skamnaki, V. T.; Bischoff, H.; Goldman, S.; Schram, M.; Watson, K. A.; Johnson, L. N. *Structure* **1997**, *5*, 1413.
12. Gregoriou, M.; Noble, M. E. M.; Watson, K. A.; Garman, E. F.; Krulle, T. M.; Fuente, C.; Fleet, G. W. J.; Oikonomakos, N. G.; Johnson, L. N. *Protein Sci.* **1998**, *7*, 915.
13. Martin, W. H.; Hoover, D. J.; Armento, S. J.; Stock, I. A.; McPherson, R. K.; Danley, D. E.; Stevenson, R. W.; Barrett, E. J.; Treadway, J. L. *Proc. Natl. Acad. Sci. U.S.A.* **1998**, *95*, 1776.
14. Hoover, D. J.; Lefkowitz-Snow, S.; Burgess-Henry, J. L.; Martin, W. H.; Armento, S. J.; Stock, I. A.; McPherson, R. K.; Genereux, P. E.; Gibbs, E. M.; Treadway, J. L. *J. Med. Chem.* **1998**, *41*, 2934.
15. Oikonomakos, N. G.; Tsitsanou, K. E.; Zographos, S. E.; Skamnaki, V. T.; Goldmann, S.; Bischoff, H. *Protein Sci.* **1999**, *8*, 1930.
16. Oikonomakos, N. G.; Zographos, S. E.; Skamnaki, V. T.; Tsitsanou, K. E.; Johnson, L. N. *J. Biol. Chem.* **2000**, *275*, 34566.
17. Oikonomakos, N. G.; Skamnaki, V. T.; Tsitsanou, K. E.; Gavalas, N. G.; Johnson, L. N. *Structure* **2000**, *8*, 575.
18. Rath, V. L.; Ammirati, M.; Danley, D. E.; Ekstrom, J. L.; Gibbs, E. M.; Hynes, T. R.; Mathiowetz, A. M.; McPherson, R. K.; Olson, T. V.; Treadway, J. L.; Hoover, D. J. *Chem. Biol.* **2000**, *7*, 677.
19. Tsitsanou, K. E.; Oikonomakos, N. G.; Zographos, S. E.; Skamnaki, V. T.; Gregoriou, M.; Watson, K. A.; Johnson, L. N.; Fleet, G. W. J. *Protein Sci.* **1999**, *8*, 741.
20. Ösz, E.; Somsák, L.; Szilágyi, L.; Kovács, L.; Docsa, T.; Tóth, B.; Gergely, P. *Bioorg. Med. Chem. Lett.* **1999**, *9*, 1385.
21. Somsák, L.; Kovács, L.; Tóth, M.; Ösz, E.; Szilágyi, L.; Györgydeák, Z.; Dinya, Z.; Docsa, T.; Tóth, B.; Gergely, P. *Chem. Eur. J.* **2001**, *44*, 2843.
22. Somsák, L.; Nagy, V. *Tetrahedron: Asymmetry* **2000**, *11*, 1719 (*Tetrahedron: Asymmetry* corrigendum: *11*, 2247)..
23. Somsák, L.; Nagy, V.; Docsa, T.; Tóth, B.; Gergely, P. *Tetrahedron: Asymmetry* **2000**, *11*, 405.
24. Martin, J. L.; Withers, S. G.; Johnson, L. N. *Biochemistry* **1990**, *29*, 10745.

25. Collaborative Computational Project *Acta Crystallogr*. **1994**, *D50*, 760.
26. Fischer, E. H.; Krebs, E. G. *Methods Enzymol*. **1962**, *5*, 369.
27. Leatherbarrow, R. J. *GraFit Version 3.0*.; Erithakus Software: Staines, UK, 1992.
28. Oikonomakos, N. G.; Melpidou, A. E.; Johnson, L. N. *Biochim. Biophys. Acta* **1985**, *832*, 248.
29. Otwinowski, Z.; Minor, W. *Methods Enzymol*. **1997**, *276*, 307.
30. Brunger, A. T. *X-PLOR Version 3.1. A System for X-ray Crystallography and NMR*. Yale University Press: New Haven, CT, 1992.
31. Read, R. J. *Acta Crystallogr*. **1986**, *A42*, 140.
32. Jones, T. A.; Zou, J. Y.; Cowan, S. W.; Kjeldgaard, M. *Acta Crystallogr*. **1991**, *A47*, 110.
33. Luzatti, V. *Acta Crystallogr*. **1952**, *5*, 802.
34. Laskowski, R. A.; MacArthur, M. W.; Moss, D. S.; Thornton, J. M. *J. Appl. Crystallogr*. **1993**, *26*, 283.